Asymptotic analysis for steady mode III crack growth in a piezoelectric sandwich composite

Zhou, Zhi Dong

Nishioka, Toshihisa

Asymptotic analysis for steady mode III crack growth in a piezoelectric sandwich composite

Zhi_Dong Zhou [1] **and Toshihisa Nishioka** [2*]

[1] Department of Engineering Mechanics, Shanghai Jiaotong University, Shanghai 200240, PR China
[2] Simulation Engineering Laboratory, Department of Ocean Mechanical Engineering,
Faculty of Maritime and Sciences, Kobe University, Kobe, 658-0022, Japan

Abstract

In this paper a steady semi-infinite mode III crack growth along the midplane of a piezoelectric layer sandwiched between two identical half spaces is considered. The Fourier integral transform is used to reduce the mixed boundary value problem to the Wiener-Hopf equation by introducing an auxiliary function. The complete stress and displacement distributions along the crack line can be obtained and further the dynamic stress and electric displacement intensity factors and the energy release rate are presented in explicit form. The results show that the crack propagation speed and coupled material constants influence on the dynamic stress and electric displacement intensity factors, moreover the dynamic energy release rate is dependent on the crack propagation speed and material 2 for this geometry.

Keywords Crack growth, Dynamic field intensity factors, Piezoelectric materials, Sandwich composite, Wiener-Hopf equation

1. Introduction

Piezoelectric ceramics are widely used as smart materials owing to their large coupling between electric and mechanical fields. In the past decade many researchers draw their attentions to the studies of stationary crack problems in piezoelectric materials under variant mechanical and electric boundary conditions and obtained significant achievements.

Due to the uncoupling of mechanical and electric fields and the simplicity in mathematics, mode III crack problems in piezoelectric materials have been analyzed by many researchers [1-3]. Recently mode III crack problems in piezoelectric strip or sandwich composite materials have become intensive topic, subjected to the static or dynamic mechanical and electric loadings. Shindo et al. [4-5], Li and Duan [6] and Li [7] considered the problems of a central crack and two collinear cracks contained in infinite piezoelectric strips by a numerical scheme and an analytic method, respectively. In addition, Li and Fan [8] studied the transient analysis of a cracked piezoelectric strip subjected to anti-plane impact loads by integral transform techniques and obtained the closed-form solutions for the dynamic field intensity factors and energy release rate in the Laplace transform domain.

There are few works devoted to the dynamic crack growth in piezoelectric materials.

*Corresponding: Phone & Fax: +81-78-431-6268,
E-mail: Nishioka@maritime.kobe-u.ac.jp

The anti-plane piezoelectric fracture problem is very important and interesting in practical engineering, because it has both mathematical simplicity and interesting physics. Dynamic crack extension is a process of crack surface growth, which relates to surface wave characteristics. Li and Mataga [9-10] considered the transient response of a semi-infinite, anti-plane crack growth in unbounded piezoelectric materials under impact loads. They obtained a special closed-form solution for constant speed crack growth under two electric boundary conditions on the crack surfaces. Chen and Yu [11] studied the Yoffe crack problem in piezoelectric materials under anti-plane mechanical and in-plane electric loadings based on the impermeable-crack assumption and showed that the stress intensity factor and electric displacement are independent of the crack growth speed. Kwon et al. [12-13] considered the cases of moving Yoffe crack in piezoelectric strip and moving Giffith eccentric crack in a piezoelectric strip bonded between two elastic materials subjected to anti-plane mechanical and in-plane electric loadings, respectively. Their results showed that the crack growth speed influences the dynamic energy release rate and also predicted the initial crack branching angle for the piezoelectric-elastic composite materials.

In practical engineering, the case of steady crack growth is considered when the crack growth in a real material is indeed steady for a long enough time that results are useful. In addition, the progress of the study of steady crack growth can be used to analyze crack growth at nonuniform rates. In this paper, we consider the steady mode III crack propagating along the midplane of a piezoelectric layer sandwiched between two identical half piezoelectric materials. By applying the Fourier integral transform method, the mixed boundary problem can be reduced to the classical Wiener-Hopf equation. Since the complete forms of stress and displacement can be presented along the real axis and the dynamic stress and electric displacement intensity factors and energy release rate can be obtained in closed-form. The results show that the dynamic stress and electric displacement intensity factors near the moving crack tip depend on the crack propagation speed and the properties of two piezoelectric materials, but dynamic energy release rate is only dependent on the crack propagation speed and material 2 for this geometry.

2. Basic equations of the problem

In this section, we consider the case of the steady mode III crack growth along the midplane of piezoelectric layer sandwiched between two identical half piezoelectric materials. As shown in Fig. 1, a semi-infinite crack located at $X<0$, $Y=0$ in material 1 initially, where the poling direction is along with Z axis and half of layer thickness is h. The half space piezoelectric material is defined as material 2, where the poling direction is along with Z axis. The crack propagates along the X axis at the constant speed v. Due to the symmetry of this problem, in this paper only the following domain need to be considered: $-\infty < X < \infty$, $Y > 0$. In this mode III crack growth problem, there are out-of-plane displacement $w(X,Y,Z,t)$ and electric potential $\phi(X,Y,Z,t)$, which

depend on X, Y and time *t*. The anti-plane strains γ_{zx}, γ_{zy} and inplane electric fields E_x, E_y are

$$\gamma_{zx} = \frac{\partial w}{\partial X}, \quad \gamma_{zy} = \frac{\partial w}{\partial Y}, \quad E_x = -\frac{\partial \phi}{\partial X}, \quad E_y = -\frac{\partial \phi}{\partial Y} \tag{1}$$

In this case, the constitutive equations can be written as

$$\tau_{zx} = c_{44}\gamma_{zx} - e_{15}E_x, \qquad \tau_{zy} = c_{44}\gamma_{zy} - e_{15}E_y$$

$$D_x = e_{15}\gamma_{zx} + \varepsilon_{11}E_x, \qquad D_y = e_{15}\gamma_{zy} + \varepsilon_{11}E_y \tag{2}$$

where τ_{yz}, τ_{xz} are shear stresses, D_y, D_x are in-plane electric displacements, and $c_{44}, e_{15}, \varepsilon_{11}$ are elastic, piezoelectric and dielectric constants, respectively. From Eqs. (1) and (2), the basic dynamic anti-plane governing equations for piezoelectric materials can be written as

$$\begin{matrix} c_{44}^{(i)}\nabla^2 w^{(i)} + e_{15}^{(i)}\nabla^2\phi = \rho^{(i)}\partial^2 w^{(i)}/\partial t^2 \\ e_{15}^{(i)}\nabla^2 w^{(i)} - \varepsilon_{11}^{(i)}\nabla^2\phi^{(i)} = 0 \end{matrix}, \quad i=1,2 \tag{3}$$

where (*i*) denotes the material 1 and material 2, $\rho^{(i)}$ is the mass density of material *i*, and $\nabla^2 = \partial^2/\partial X^2 + \partial^2/\partial Y^2$ is the two-dimensional Laplacian operator.

When the semi-infinite crack propagates along the *X* axis at a constant speed *v*, we can introduce the new local Cartesian coordinates *x*-*y* located at the moving crack tip

$$x = X - vt, \qquad y = Y, \tag{4}$$

So in new coordinate, Eq. (3) can be rewritten as

$$\begin{matrix} \alpha_{(i)}^2 \frac{\partial^2}{\partial x^2} w^{(i)}(x,y) + \frac{\partial^2}{\partial y^2} w^{(i)}(x,y) = 0 \\ \nabla^2 \varphi^{(i)}(x,y) = 0 \end{matrix} \tag{5}$$

in which the new Bleustein function $\varphi^{(i)}$ is introduced [14]

$$\varphi^{(i)} = \phi^{(i)} - \frac{e_{15}^{(i)}}{\varepsilon_{11}^{(i)}} w^{(i)}, \quad i=1,2 \tag{6}$$

and

$$\alpha_{(i)}^2 = 1 - (v/c^{(i)})^2, \quad c^{(i)} = \sqrt{c_e^{(i)}/\rho^{(i)}}, \quad c_e^{(i)} = c_{44}^{(i)} + (e_{15}^{(i)})^2/\varepsilon_{11}^{(i)} \tag{7}$$

where $\alpha_{(i)}$ is the nondimensional parameter of material *i*, $c^{(i)}$ is the speed of the piezoelectrically stiffened bulk shear wave of material *i*, and $c_e^{(i)}$ is the piezoelectrically stiffened elastic constant of material *i*, respectively.

Using the functions $w^{(i)}$ and $\varphi^{(i)}$, the piezoelectric constitutive equations can be re-expressed as

$$\tau_{xz}^{(i)}(x,y) = c_e^{(i)} \frac{\partial w^{(i)}}{\partial x} + e_{15}^{(i)} \frac{\partial \varphi^{(i)}}{\partial x}, \qquad \tau_{yz}^{(i)}(x,y) = c_e^{(i)} \frac{\partial w^{(i)}}{\partial y} + e_{15}^{(i)} \frac{\partial \varphi^{(i)}}{\partial y},$$

$$D_x^{(i)}(x,y) = -\varepsilon_{11}^{(i)} \frac{\partial \varphi^{(i)}}{\partial x}, \qquad D_y^{(i)}(x,y) = -\varepsilon_{11}^{(i)} \frac{\partial \varphi^{(i)}}{\partial y}. \tag{8}$$

At the crack plane, mechanical boundary conditions along the crack line can be expressed as

$$w^{(1)}(x,0) = 0 \quad , \quad x>0 \tag{9a}$$

$$\tau_{yz}^{(1)}(x,0) = q(x) \quad , \quad x<0 \tag{9b}$$

where $q(x)$ is a known stress loading function along the crack surface. However, there are some different electric boundary conditions along the crack surface: impermeable-crack assumption that regards the crack as a hole full of vacuum or air which related permittivity is close to 1 and permeable-crack assumption that regards normal electric displacement and tangent electric field are continuous across the crack surfaces. The permeable-crack assumption has the physical reasonableness for anti-plane crack. Following the discussion of Li and Duan [6], the permeable-crack electric boundary condition along the crack line can be written as

$$\phi^{(1)}(x,0) = 0 \quad , \quad -\infty < x < \infty \tag{10a}$$

$$D_y^{(1)}(x,0) = D_0(x), \quad x<0 \tag{10b}$$

where $D_0(x)$ is a know electric displacement load along the crack surface. So Eqs. (9) and (10) propose a mixed boundary-value problem.

At the interface of the layer and the half-space piezoelectric material, displacement, electric potential, normal electric displacement and shear stress are continuous across the interface, i.e.

$$w^{(1)}(x,h) = w^{(2)}(x,h) \quad , \quad -\infty < x < \infty \tag{11a}$$

$$\phi^{(1)}(x,h) = \phi^{(2)}(x,h) \quad , \quad -\infty < x < \infty \tag{11b}$$

$$D_y^{(1)}(x,h) = D_y^{(2)}(x,h) \quad , \quad -\infty < x < \infty \tag{11c}$$

$$\tau_{yz}^{(1)}(x,h) = \tau_{yz}^{(2)}(x,h) \quad , \quad -\infty < x < \infty \tag{11d}$$

In this case, the remote stress and electric displacement vanish, i.e.

$$\tau_{yz}^{(i)}(x,y), D_y^{(i)}(x,y) \to 0 \quad \text{, when } \ \mathrm{x} < 0, \mathrm{y} \neq 0 \ \text{ and } \ \sqrt{x^2 + y^2} \to \infty \tag{12}$$

3. Integral equation solutions

In this section, the Fourier integral transform equation is applied to solve the above mixed boundary value problem. The Fourier integral transform and inverse transform are

$$\bar{f}(\lambda, y) = \int_{-\infty}^{\infty} f(x,y) e^{i\lambda x} dx \,, \qquad f(x,y) = \frac{1}{2\pi} \int_{-\infty}^{\infty} \bar{f}(\lambda, y) e^{-i\lambda x} d\lambda \tag{13}$$

From Eqs. (5) and (13), the displacements and Bleustein functions can be expressed as follows:

$$w^{(1)}(x,y) = \frac{1}{2\pi} \int_{-\infty}^{\infty} [A_1^{(1)}(\lambda) e^{\lambda \alpha_{(1)} y} + A_2^{(1)} e^{-\lambda \alpha_{(1)} y}] e^{-i\lambda x} d\lambda \tag{14a}$$

$$\varphi^{(1)}(x,y) = \frac{1}{2\pi} \int_{-\infty}^{\infty} [B_1^{(1)}(\lambda) e^{\lambda y} + B_2^{(1)} e^{-\lambda y}] e^{-i\lambda x} d\lambda \tag{14b}$$

$$w^{(2)}(x,y) = \frac{1}{2\pi} \int_{-\infty}^{\infty} [A_1^{(2)}(\lambda) e^{-|\lambda| \alpha_{(2)} y}] e^{-i\lambda x} d\lambda \tag{14c}$$

$$\varphi^{(2)}(x,y) = \frac{1}{2\pi} \int_{-\infty}^{\infty} [B_1^{(2)}(\lambda) e^{-|\lambda| y}] e^{-i\lambda x} d\lambda \tag{14d}$$

where $A_1^{(1)}, A_2^{(1)}, B_1^{(1)}, B_2^{(1)}, A_1^{(2)}, B_1^{(2)}$ are the unknown functions of λ to be solved. Substituting Eq. (14) into Eqs. (10a) and (11), along the interface the shear stress and displacement can be expressed in Fourier integral forms

$$\bar{\tau}_{yz}^{(1)}(\lambda,0) = A(\lambda) A_1^{(1)}, \ \ \bar{w}^{(1)}(\lambda,0) = B(\lambda) A_1^{(1)}, \ \ \bar{D}_y^{(1)}(\lambda,0) = C(\lambda) A_1^{(1)},$$

$$\bar{\tau}_{yz}^{(1)}(\lambda,0) = G(\lambda) \bar{w}^{(1)}(\lambda,0) \tag{15}$$

where $A(\lambda), B(\lambda)$ and $C(\lambda)$ are very complicated and not listed here and $G(\lambda)$ is an auxiliary function and written as

$$G(\lambda) = \frac{\bar{\tau}_{yz}^{(1)}(\lambda,0)}{\bar{w}^{(1)}(\lambda,0)} = -|\lambda| \frac{M(\lambda)}{N(\lambda)} \tag{16}$$

where

$$M(\lambda) = t_1 \sinh(h\lambda)\sinh(h\alpha_{(1)}\lambda) + t_2 \cosh(h\,|\,\lambda\,|)\sinh(h\alpha_{(1)}\,|\,\lambda\,|) + t_3 \sinh(h\,|\,\lambda\,|)\cosh(h\alpha_{(1)}\,|\,\lambda\,|)$$
$$+ t_4 \cosh(h\lambda)\cosh(h\alpha_{(1)}\lambda) + t_5$$

$$N(\lambda) = \varepsilon_{11}^{(1)}(c_e^{(1)}\alpha_{(1)}\varepsilon_{11}^{(1)^2}\varepsilon_{11}^{(2)} \cosh(h\lambda)\cosh(h\alpha_{(1)}\lambda) + c_e^{(1)}\alpha_{(1)}\varepsilon_{11}^{(1)}\varepsilon_{11}^{(2)^2} sihh(h\,|\,\lambda\,|)\cosh(h\alpha_{(1)}\,|\,\lambda\,|)$$
$$+ c_e^{(2)}\alpha_{(2)}\varepsilon_{11}^{(1)}\varepsilon_{11}^{(2)^2} \sinh(h\lambda)\sinh(h\alpha_{(1)}\lambda) + t_6 \cosh(h\,|\,\lambda\,|)\sinh(h\alpha_{(1)}\,|\,\lambda\,|))$$

(17)

where

$$t_1 = e_{15}^{(1)^2} e_{15}^{(2)^2} \varepsilon_{11}^{(1)^2} - e_{15}^{(1)^2} \varepsilon_{11}^{(1)} \varepsilon_{11}^{(2)} (2e_{15}^{(1)} e_{15}^{(2)} + c_e^{(2)} \alpha_{(2)} \varepsilon_{11}^{(1)}) + \varepsilon_{11}^{(2)^2} (e_{15}^{(1)^4} + c_e^{(1)^2} \alpha_{(1)}^2 \varepsilon_{11}^{(1)^2})$$

$$t_2 = c_e^{(1)^2} \alpha_{(1)}^2 \varepsilon_{11}^{(1)^3} \varepsilon_{11}^{(2)} - c_e^{(2)} \alpha_{(2)} \varepsilon_{11}^{(1)} \varepsilon_{11}^{(2)^2} e_{15}^{(1)^2}$$

$$t_3 = c_e^{(1)} c_e^{(2)} \alpha_{(1)} \alpha_{(2)} \varepsilon_{11}^{(1)^2} \varepsilon_{11}^{(2)^2} - c_e^{(1)} \alpha_{(1)} e_{15}^{(1)^2} \varepsilon_{11}^{(1)^2} \varepsilon_{11}^{(2)}$$

$$t_4 = c_e^{(1)} \alpha_{(1)} \varepsilon_{11}^{(1)} (\varepsilon_{11}^{(1)} \varepsilon_{11}^{(2)} (2e_{15}^{(1)} e_{15}^{(2)} + c_e^{(2)} \alpha_{(2)} \varepsilon_{11}^{(1)}) - e_{15}^{(2)^2} \varepsilon_{11}^{(1)^2} - 2e_{15}^{(1)^2} \varepsilon_{11}^{(2)^2})$$

$$t_5 = 2c_e^{(1)} \alpha_{(1)} e_{15}^{(1)} \varepsilon_{11}^{(1)} \varepsilon_{11}^{(2)} (e_{15}^{(1)} \varepsilon_{11}^{(2)} - e_{15}^{(2)} \varepsilon_{11}^{(1)})$$

$$t_6 = t_4 / c_e^{(1)} \alpha_{(1)} \varepsilon_{11}^{(1)} + e_{15}^{(1)^2} \varepsilon_{11}^{(2)^2}$$

Here mechanical boundary conditions in Eqs. (9a) and (9b) are expanded over full range of *x*-axis. The shear stress and displacement along full rang of *x*-axis are rewritten as

$$w^{(1)}(x,0) = w_-(x) + 0 \quad , \quad -\infty < x < \infty \tag{18a}$$

$$\tau_{yz}^{(1)}(x,0) = \tau_+(x) + \tau_-(x) \quad , \quad -\infty < x < \infty \tag{18b}$$

where

$$w_-(x) = \begin{cases} 0 & x > 0 \\ w^{(1)}(x,0) & x < 0 \end{cases} \tag{19a}$$

$$\tau_+(x) = \begin{cases} \tau_{yz}^{(1)}(x,0) & x > 0 \\ 0 & x < 0 \end{cases} \tag{19b}$$

$$\tau_-(x) = \begin{cases} 0 & x > 0 \\ q(x) & x < 0 \end{cases} \tag{19c}$$

Along the crack line, the shear stress and displacement in Fourier integral forms are

$$\begin{aligned}\overline{\tau}_{yz}^{(1)}(\lambda,0) &= \int_{-\infty}^{\infty}\tau_{yz}^{(1)}(x,0)e^{i\lambda x}dx = \int_{-\infty}^{0}\tau^{-}(x)e^{i\lambda x}dx + \int_{0}^{\infty}\tau^{+}(x)e^{i\lambda x}dx \\ \overline{w}^{(1)}(\lambda,0) &= \int_{-\infty}^{\infty}w^{(1)}(x,0)e^{i\lambda x}dx = \int_{-\infty}^{0}w^{-}(x)e^{i\lambda x}dx + \int_{0}^{\infty}w^{+}(x)e^{i\lambda x}dx\end{aligned} \tag{20}$$

From Eq. (20), it is obvious that the first integral at the right side of equations is regular as $\mathrm{Im}(\lambda) \le 0$ and the second integral at the right side of equations is regular as $\mathrm{Im}(\lambda) \ge 0$. So Eq. (20) can be simplified as

$$\begin{aligned}\overline{\tau}_{yz}^{(1)}(\lambda,0) &= \tau^{-}(\lambda) + \tau^{+}(\lambda) \\ \overline{w}^{(1)}(\lambda,0) &= w^{-}(\lambda) + w^{+}(\lambda) = w^{-}(\lambda)\end{aligned} \tag{21}$$

where superscript "+" and "-" denote the functions regular in the upper ($\mathrm{Im}(\lambda) \ge 0$) and lower ($\mathrm{Im}(\lambda) \le 0$) half spaces, respectively. For $\mathrm{Im}(\lambda) = 0$, substitute Eq. (15) into Eq. (21) and get the Wiener-Hopf equation

$$\tau^{+}(\lambda) = G(\lambda)w^{-}(\lambda) - \tau^{-}(\lambda) \quad , \qquad \mathrm{Im}(\lambda) = 0 \tag{22}$$

For the further deduction using Fourier integral transform, we chose the decaying loading function $q(x)$ as the following

$$q(x) = -q_0 \exp(x/l) \tag{23}$$

where l is a length parameter expressing the loading decay rate. So we can get

$$\tau^{-}(\lambda) = \int_{-\infty}^{0} q(x)e^{i\lambda x}dx = \frac{iq_0}{(\lambda - i/l)} \tag{24}$$

The Wiener-Hopf procedure requires $G(\lambda)$ be factored into the product of sectionally analytic functions, i.e.

$$G(\lambda) = G^{+}(\lambda)G^{-}(\lambda) \tag{25}$$

where $G^{+}(\lambda)$ is regular in $\mathrm{Im}(\lambda) \ge 0$ and $G^{-}(\lambda)$ is regular in $\mathrm{Im}(\lambda) \le 0$. The function $G(\lambda)$ is very complicated, but we only need to obtain its behavior for large $|\lambda|$ and small $|\lambda|$. From Eqs. (16) and (17), we can get

$$G(\lambda) \sim \begin{cases} -(c_e^{(2)}\alpha_{(2)} - e_{15}^{(2)^2}/\varepsilon_{11}^{(2)}) \mid \lambda \mid = -\mu_{(2)} \mid \lambda \mid, & \mid \lambda \mid \to 0 \\ -(c_e^{(1)}\alpha_{(1)} - e_{15}^{(1)^2}/\varepsilon_{11}^{(1)}) \mid \lambda \mid = -\mu_{(1)} \mid \lambda \mid, & \mid \lambda \mid \to \infty \end{cases} \tag{26}$$

where the symbol "~" denotes asymptotic convergence. This equation is very similar to that of Ryvkin [15] and $G(\lambda)$ for large and small $|\lambda|$ can be regarded as properties of the piezoelectric layer and piezoelectric half space, respectively. From Eq. (26), we define a new function $K(\lambda)$ as

$$K(\lambda) = \frac{G(\lambda)}{-\mu_{(1)} \mid \lambda \mid} = K^{+}(\lambda)K^{-}(\lambda) \quad , \quad \mathrm{Im}(\lambda) = 0 \tag{27}$$

where

$$K(\lambda) = 1 + O(\lambda^{-1}) \quad , \quad \lambda \to \infty \tag{28}$$

By means of Cauchy's integral theorem, we can get

$$\begin{aligned} \ln K^{+} &= \frac{1}{2\pi i}\int_{-\infty}^{\infty} \frac{\ln K(z)}{z-\lambda} dz \quad , \quad \mathrm{Im}(\lambda) > 0 \\ \ln K^{-} &= -\frac{1}{2\pi i}\int_{-\infty}^{\infty} \frac{\ln K(z)}{z-\lambda} dz \quad , \quad \mathrm{Im}(\lambda) < 0 \end{aligned} \tag{29}$$

so that

$$K^{\pm}(\lambda) = \exp\left\{\frac{\pm 1}{2\pi i}\int_{-\infty}^{\infty} \frac{\ln K(z)}{z-\lambda} dz\right\} \tag{30}$$

where $K^{\pm}(\lambda)$ are not only analytic but also nonzero in the respective half planes, so $K^{\pm}(\lambda)$ and $\ln K^{\pm}(\lambda)$ have the same analytic domain.

Substituting Eqs. (24), (27) and (30) into the Wiener-Hopf equation (22), it is given

$$\begin{aligned} &\frac{\tau^{+}(\lambda)}{K^{+}(\lambda)\sqrt{\lambda + i0}} + \frac{iq_0}{(\lambda - i/l)}\left(\frac{1}{K^{+}(\lambda)\sqrt{\lambda + i0)}} - \frac{1}{K^{+}(i/l)\sqrt{i/l + i0}}\right) = \\ &-(\mu_{(1)}K^{-}(\lambda)\sqrt{\lambda - i0}w^{-}(\lambda) + \frac{iq_0}{(\lambda - i/l)}\frac{1}{K^{+}(i/l)\sqrt{i/l + i0}}) \end{aligned} \tag{31}$$

where $\lambda + i0$ and $\lambda - i0$ express λ approaching to the real axis along the positive and negative imaginary axes, respectively, and $\sqrt{\lambda}$ takes singular value in the λ-plane cut along the negative real axis. Eq. (31) is valid on the real axis and each side of equation is analytic in the respective half planes. Based on the generalized Liouville theorem and additional assumption of the bounded local strain energy, we can get a

complete solution of the Wiener-Hopf equation.

$$\tau^{+}(\lambda)=\frac{iq_0}{(\lambda-i/l)}\left(\frac{K^{+}(\lambda)\sqrt{\lambda+i0}}{K^{+}(i/l)\sqrt{i/l+i0}}-1\right)$$
$$w^{-}(\lambda)=-\frac{iq_0}{(\lambda-i/l)}\frac{1}{\mu_{(1)}K^{-}(\lambda)\sqrt{\lambda-i0}K^{+}(i/l)\sqrt{i/l+i0}} \tag{32}$$

So from Eqs. (14), (15), (16), (17), (27), (30) and (32), the complete closed-form solutions for mode III crack growth can be obtained.

4. The field intensity factors and energy release rate near the crack tip

Due to the complicity of the auxiliary $G(\lambda)$ (or $K(\lambda)$), here only the singular fields of stress and displacement are considered. Just the same as in recent work [16], the shear loading is assumed as

$$q_0=\frac{K_0}{\sqrt{l}} \tag{33}$$

where K_0 is an arbitrary constant having the dimensions of stress intensity factor and

$$K_0=\frac{c_e^{(1)}}{c_{44}^{(1)}}\tau_0\left[1-\left(\frac{c_{44}^{(1)}e_{15}^{(1)}}{c_e^{(1)}\varepsilon_{11}^{(1)}}\frac{D_0}{\tau_0}\right)\right] \tag{34}$$

where τ_0 is the modulus of pure mechanical shear stress at zero electric load and D_0 is the modulus of electric displacement load along the crack surface, respectively. When $l\to\infty$, in Eq. (23) the shear stress function approaches to zero and there is a traction-free condition on the crack surfaces, but the mechanical and electric fields in the body do not become to zero and are proportional to K_0. As the discussion of Ryvkin [15] "This limiting distribution, proportional to *p*, which may be viewed as generated by the remote stresses applied at infinity…", here is the same case.

When $l\to\infty$ in this paper, with the aid of Eq. (33), Eq. (32) can be reduced to

$$\tau^{+}(\lambda)=\frac{K_0K^{+}(\lambda)}{K^{+}(0)\sqrt{\lambda+i0}}e^{\frac{\pi}{4}i}$$
$$w^{-}(\lambda)=-\frac{K_0}{\mu_{(1)}K^{+}(0)K^{-}(\lambda)(\lambda-i0)^{3/2}}e^{\frac{\pi}{4}i} \tag{35}$$

With the inverse Fourier transform integral, the complete forms of stress and displacement along the crack line can be expressed as

$$\begin{cases} \tau_{yz}^{(1)}(x,0) = \dfrac{1}{2\pi}\displaystyle\int_{-\infty}^{\infty} \tau^{+}(\lambda) e^{-i\lambda x} d\lambda \\ w^{(1)}(x,0) = \dfrac{1}{2\pi}\displaystyle\int_{-\infty}^{\infty} w^{-}(\lambda) e^{-i\lambda x} d\lambda \end{cases} \tag{36}$$

In order to obtain the singular terms of the stress and displacement near the moving crack tip and far field, the following results should be given

$$\tau^{+}(\lambda) \sim \begin{cases} \dfrac{K_0}{K^{+}(0)} \dfrac{1}{\sqrt{-i\lambda}} & |\lambda| \to \infty \\ K_0 / \sqrt{-i\lambda} & \mathrm{Im}(\lambda) \to 0^{+} \end{cases} \tag{37a}$$

$$w^{-}(\lambda) \sim \begin{cases} \dfrac{K_0}{\mu_{(1)} K^{+}(0) (i\lambda)^{3/2}} & |\lambda| \to \infty \\ \dfrac{K_0}{\mu_{(2)} (i\lambda)^{3/2}} & \mathrm{Im}(\lambda) \to 0^{-} \end{cases} \tag{37b}$$

In this study, the limiting case of a large ration of the crack length to the layer thickness must be added. For the asymptotic form of stress and displacement, the cracked layer thickness is the only length parameter of the results for a sufficiently long crack in a piezoelectric sandwich composite. Application of the Abel theorem on asymptotic properties of transforms in the present situation implies

$$\begin{aligned} &\lim_{\lambda \to +\infty} (-i\lambda)^{1/2} \tau^{+}(\lambda) = \lim_{x \to 0^{+}} (\pi x)^{1/2} \tau_{yz}^{(1)}(x) \\ &\lim_{\mathrm{Im}(\lambda) \to 0^{+}} (-i\lambda)^{1/2} \tau^{+}(\lambda) = \lim_{x \to +\infty^{+}} (\pi x)^{1/2} \tau_{yz}^{(1)}(x) \end{aligned} \tag{38}$$

So the near dynamic stress intensity factors and far dynamic stress intensity factor of crack can be determined as, respectively

$$K_{III} = \lim_{x \to 0^{+}} \sqrt{2\pi x}\, \tau_{yz}^{(1)}(x,0) = \sqrt{2} K_0 / K^{+}(0) = \sqrt{2\mu_{(1)} / \mu_{(2)}}\, K_0 \tag{39a}$$

$$K_{III}^{f} = \lim_{x \to \infty} \sqrt{2\pi x}\, \tau_{yz}^{(1)}(x,0) = \sqrt{2} K_0 \tag{39b}$$

In addition, when $|\lambda|$ is approached to infinity, from Eq. (15), the following expression can be obtained

$$\overline{D}_{y}^{(1)}(\lambda,0) = \frac{e_{15}^{(1)}}{\mu_{(1)}} \overline{\tau}_{zy}^{(1)}(\lambda,0) \tag{40}$$

So the near electric displacement intensity factor of crack is given as

$$K_D = \frac{e_{15}^{(1)}}{\mu_{(1)}} K_{III} = e_{15}^{(1)} \sqrt{2/(\mu_{(1)} \mu_{(2)})}\, K_0 \tag{41}$$

The results of Eq. (39) are very similar to that of Ryvkin [15] under similar loading

except the different general constant $\mu_{(i)}$, whereas there are different deformation modes and different materials in two papers. For the piezoelectric sandwich composite, Eqs. (39) and (41) show that near dynamic field intensity factors depend on the crack propagation speed and coupled material properties and far dynamic stress intensity factor only relates to the arbitrary constant K_0. It is very obvious that the near electric displacement intensity factor increase with the increase of crack speed *v* regardless of the material combinations. When the properties of two materials become identical and the sandwich composite is an unbounded homogeneous piezoelectric body, the crack propagation speed does not influence the near stress intensity factor but influence the near electric displacement intensity factor for steady mode III crack growth. These reduced results are same as that of the previous literatures [12-13].

In this example, we consider PZT-6B as the material 1, which material properties are listed in Table 1. Figure 2 displays normalized stress intensity factor K_{III} / K_{III}^{f} versus the piezoelectric mismatch ratios $e_{15}^{(2)} / e_{15}^{(1)}$ for different dielectric mismatch ratios $\varepsilon_{11}^{(2)} / \varepsilon_{11}^{(1)}$ for a large crack propagation speed under the same elastic constants. It shows that the normalized stress intensity factor increases with the increase of the dielectric constant of material 2 and decreases with the increase of the piezoelectric constant of material 2, respectively. Figure 3 gives variations of normalized stress intensity factor for different crack propagation speeds as the same elastic constants. The result shows that the possibility of the crack propagation speed increasing or decreasing the normalized stress intensity factor depends on the material combinations. In this figure, there is a transformation point, which is dependent of the properties of materials. Further, we can find that a low crack propagation speed has little effect on the normalized stress intensity factor regardless of the material combinations.

In this case the dynamic energy release rate is defined as the change of the energy of the crack propating an infinitesimal length, and the dynamic energy release rate per unit length at the moving crack tip is given by

$$G = \lim_{\delta \to 0} \frac{1}{2\delta} \int_0^{\delta} [2\tau_{yz}^{(1)}(r,0) w^{(1)}(\delta - r) + 2D_y^{(1)}(r,0) \phi^{(1)}(\delta - r)] dr \tag{42}$$

where δ is crack extension length and *r* is the distance from the crack tip. From Eq. (10a), the second term of dynamic energy release rate is zero, so Eq. (42) reduces to the mechanical energy release rate. By using Eqs. (36), (37) and (38), the dynamic energy release rate can be rewritten as

$$G = \lim_{\delta \to 0} \frac{1}{\delta} \int_0^{\delta} [\tau_{yz}^{(1)}(r,0) w^{(1)}(\delta - r)] dr = K_0^{\,2} / \mu_{(2)} \tag{43}$$

where the following relation is applied

$$\int_0^1 \frac{\sqrt{1-x}}{\sqrt{x}} dx = \pi / 2 \tag{44}$$

When the crack propagation speed v becomes zero and sandwich composite becomes the homogeneous piezoelectric material, the result is the same as that of Zhang and Tong [2], Shindo et al. [5] and Li [7]. The Eq. (43) shows that the dynamic energy release rate is dependent on the crack propagation speed and material 2 only for this geometry.

5. Conclusions

This paper analyzes a problem of steady semi-infinite mode III crack growth along the midplane of a piezoelectric layer, which is sandwiched between two identical half spaces. The mixed boundary value problem is reduced to the Wiener-Hopf equation by introducing an auxiliary function with the aid of Fourier integral transform. The complete forms of stress and displacement distributions along the real axis can be obtained and further the dynamic field intensity factors and the energy release rate are presented in explicit form. The results show that near moving crack tip the crack propagation speed and coupled material constants influence on the dynamic stress and electric displacement intensity factors, moreover the dynamic energy release rate is dependent on the crack propagation speed and material 2 for this geometry. The results seem that the cracked piezoelectric layer thickness has no influence on the field intensity factors and the further numerical analysis of mechanical and electric fields and K-dominance zone will be discussed.

Acknowledgements

This study was supported by the Grant-in-aid for Scientific Research from the Ministry of Education, Culture, Sports, Science and Technology in Japan. We also acknowledge Prof. T. Fujimoto for his valuable discussions. Authors thank for reviewers for their available comments.

References

[1] S. Li, W. Gao, L.E. Gross, Stress and electric displacement distribution near Griffith's type III crack tips in piezoceramics. *Mater. Lett.* 10 (1990), 219-222.
[2] T. Y. Zhang, P. Tong, Fracture mechanics for a mode III crack in a piezoelectric material. *Int. J. Solids Structures* 33 (1996), 343-359.
[3] M. S. Hou, L. Y. Mei, Problems of antiplane strain of electrically-permeable interface crack between bonded dissimilar piezoelectric materials. *Chinese Sci. Bull.* 43 (1998), 341-345.
[4] Y. Shindo, F. Narita, K. Tanaka, Electroelastic intensification near anti-plane shear crack in orthotropic piezoelectric ceramic strip. *Theory Appl. Fract. Mech.* 25 (1996),

65-71.
[5] Y. Shindo, K. Tanaka, F. Narita, Singular stress and electric fields of a piezoelectric ceramic strip with a finite crack under longitudinal shear. *Acta Mech.* 120 (1997), 31-45.
[6] X. F. Li, X. Y. Duan, Closed-form solution for a mode-III crack at the mid-plane of a piezoelectric layer. *Mech. Res. Comm.* 28 (2001), 703-710.
[7] X. F. Li, Closed-form solution for a piezoelectric strip with two collinear cracks normal to the strip boundaries. *Eur. J. Mech. A/ Solids* 21 (2002), 981-989.
[8] X. F. Li, T. Y. Fan, Transient analysis of a piezoelectric strip with a permeable crack under antiplane impact loads. *Int. J. Eng. Sci.* 40 (2002), 131-143.
[9] S. Li, P. A. Mataga, Dynamic crack propagation in piezoelectric materials-Part I. electrode solution. *J. Mech. Phys. Solids* 44 (1996), 1799-1830.
[10] S. Li, P. A. Mataga, Dynamic crack propagation in piezoelectric materials-Part II. vaccum solution. *J. Mech. Phys. Solids* 44 (1996), 1831-1966.
[11] Z. T. Chen, S. W. Yu, Antiplane Yoffe crack problem in piezoelectric materials. *Int. J. Fracture* 84 (1997), 41-45.
[12] J. H. Kwon, K. Y. Lee, S. M. Kwon, Moving crack in a piezoelectric ceramic strip under anti-plane shear loading. *Mech. Res. Commum.* 27 (2000), 327-332.
[13] S. M. Kwon, H. S. Choi, K. Y. Lee, Moving eccentric crack in a piezoelectric strip bonded to elastic materials. *Arch. Appl. Mech.* 72 (2002), 160-170.
[14] J. L. Bleustein, A new surface wave in piezoelectric materials. *Appl. Phys. Lett.* 13 (1968), 412-413.
[15] M. Ryvkin, K-dominance zone for a semi-infinite mode I crack in a sandwich composite. *Int. J. Solids Structures* 37 (2000), 4825-4840.
[16] M. Ryvkin, L. Slepyan, L. Banks-Sills, On the scale effect in the thin layer delamination problem. *Int. J. Fracture* 71 (1995), 247-271.

Material	$c_{44}(\times 10^{9} N/m^{2})$	$e_{15}(C/m^{2})$	$\varepsilon_{11}(\times 10^{-9} C/Vm)$	$\rho(\times 10^{3} kg/m^{3})$
PZT-6B	27.1	4.6	3.6	7.6

Table 1. The material properties of PZT-6B piezoelectric ceramic.

Captions of Figures

Fig. 1. A growing anti-shear crack in a piezoelectric sandwich composite.

Fig. 2. Variations of the normalized stress intensity factor versus the piezoelectric mismatch ratios $e_{15}^{(2)}/e_{15}^{(1)}$ for different dielectric mismatch ratios $\varepsilon_{11}^{(2)}/\varepsilon_{11}^{(1)}$ at the crack propagation speed $v = 0.72c^{(1)}$.

Fig. 3. Variations of the normalized stress intensity factor versus the piezoelectric mismatch ratios $e_{15}^{(2)}/e_{15}^{(1)}$ for different crack propagation speeds as dielectric mismatch ratio $\varepsilon_{11}^{(2)}/\varepsilon_{11}^{(1)} = 0.1$.

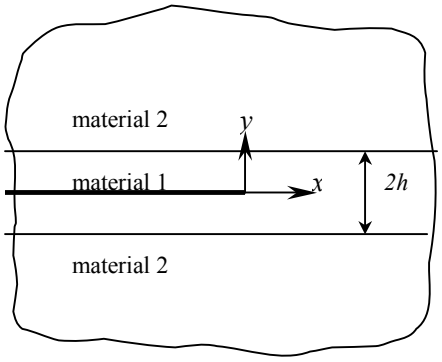

Fig. 1. A growing anti-shear crack in a piezoelectric sandwich composite.

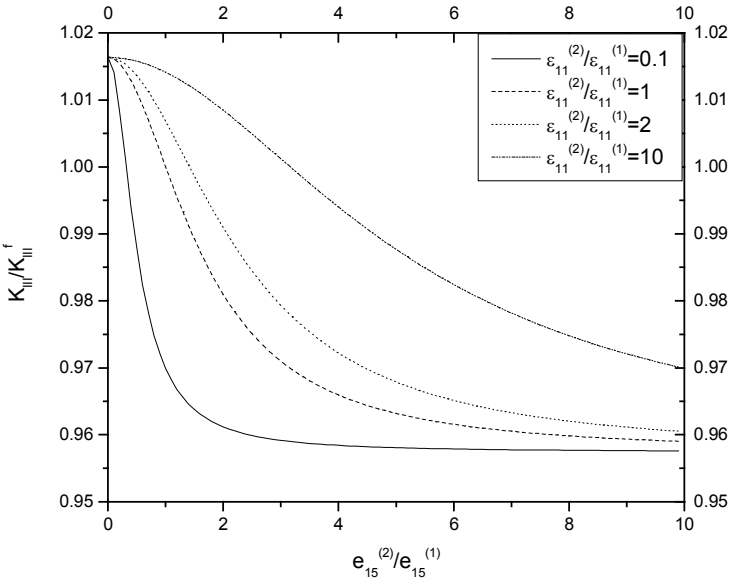

Fig. 2. Variations of the normalized stress intensity factor versus the piezoelectric mismatch ratios $e_{15}^{(2)} / e_{15}^{(1)}$ for different dielectric mismatch ratios $\varepsilon_{11}^{(2)} / \varepsilon_{11}^{(1)}$ at the crack propagation speed $v = 0.72c^{(1)}$.

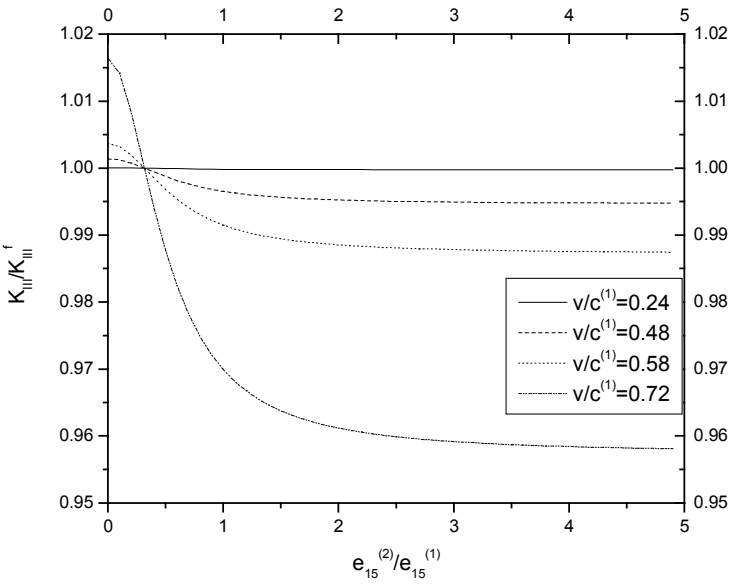

Fig. 3. Variations of the normalized stress intensity factor versus the piezoelectric mismatch ratios $e_{15}^{(2)} / e_{15}^{(1)}$ for different crack propagation speeds as dielectric mismatch ratio $\varepsilon_{11}^{(2)} / \varepsilon_{11}^{(1)} = 0.1$.